UNIVERSITE KASDI MERBAH OUARGLA

Faculty of Applied Sciences

Department of Mechanical Engineering

Submitted for the Diploma of Master

Specialty: Mechanical Engineering

Option: Energetics

Theme

Simplified dynamic simulation for solar flat plate parametric studies

Presented by:

Benchabana Mohammedkarim

In front of the Jury composed of

Président	**Mr. Ashouri Al-Haj**	**U. Kasdi Merbah Ouargla**
Examinateur	**Mrs. Bakhalid Yamna**	**U. Kasdi Merbah Ouargla**
Supervisor	**Mr. Kina Mohammed Salah**	**U. Kasdi Merbah Ouargla**

Academic year: 2024/2025

Recognition

First and foremost, I give thanks to Almighty God, who gave me the strength, patience, and perseverance necessary to complete this work. It is because of His will that I was able to acquire some consistency and take each step of this project.

I would like to express my gratitude to all those who, in one way or another, contributed to the completion of my thesis, regardless of how big or small their role was. This journey has been a valuable experience for me.

A special thank you to Dr. Kina Mohamed Salah for her thoughtful guidance, availability, expertise, and valuable support throughout this work. Her scientific rigor, her kindness, and her confidence in the necessary foundations of this project.

I would also like to thank the members of the jury who agreed to review this thesis and whose observations and comments will undoubtedly contribute to the development of my future project.

I would also like to express my sincere gratitude to all the instructors in the Mechanical Engineering Department at Kasdi Merbah University in Ouargla for the excellence of their teaching and their commitment.

Thank you to all those who helped, motivated, and encouraged me throughout this work. The Church of Lüttringhausen also supported its members as they worked, etc.

Dédicaces

I dedicate this modest work

to my mother, ***Nadia Ben Hamida****, my source of inspiration*

and to my father, ***zohir****, source of my respect, as a token of my deep gratitude*

for all his efforts and support.

To my brothers, ***said****,* ***elhachmi****,* ***firouz****,* ***imane***

To the ***Benchabana*** *family*

A special dedication to my colleagues and friends

Hassane noune*,* ***Trabelsi Taha***

*Supervisor****: Dr. Kena Mohammed Salah****, may God help you to have health, happiness and a long life.*

To all the friends who helped and encouraged me during my years of study.

Finally, I dedicate this work to all my colleagues and friends in the department.

Mechanical Engineering 2024/2025

Mohammedkarim benchabana

SUMMARY

Recognition II
Dédicaces III
List of Figures V
List of tables V
List of Graphs V
Summary: VI
Nomenclature : VII
General Introduction: 2
Chapter I: Overview of Solar Thermal Systems 3
1. Introduction 4
1.1 Theoretical Bases: 4
1.2 Flat-Plate Collectors: 4
1.2.1 Operating Principle of a Flat-Plate Solar Thermal Collector: 4
1.2.2 The principle of flat plate collector 4
1.2.3 Glazed Flat Collector: 5
1.3 Different Components of the Solar Collector: 6
1.3.1 The Absorber: 6
1.3.2 The Transparent Cover: 6
1.3.3 The Thermal Insulator: 6
1.3.4 The Heat Transfer Fluid: 7
1.3.5 Tilt of a Solar Collector 7
1.4 Types Solar Water Collector 8
1.4.1 Advantages and Disadvantages of Glazed Flat Collectors: 8
1.4.2 Efficiency of a Solar Collector 9
1.5 Bibliographic Studies 9
1.6 Materials and Methods 11
Conclusion: 12
Chapter II: Simulation model of the solar flat plate 13
2. Numerical modeling of the active solar heting systems 14
2.1 The single glazing flat plate solar colector 14
2.1.1 Temperature calculations, ... 14
2.1.2 Model of the heated envelope 16
2.1.3 Model development and Assumptions 17
2.2 Numerical application: 23
Conclusion: 26
Chapter III: Results and Discussions 27
3. Results and Discussions: 28
GENERAL CONCLUSION 32
Reference 34

List of Figures

Figure I.1a: Schematic of a plate solar collector with transparent screens 05
Figure I.1b: Components of solar flat plate collector 05
Figure I.2: Laser welding absorber. 06
Figure I.2a: Single glazed flat plate solar panel temperature distribution. 11
Figure I.2b: Single glazed flat plate solar panel heat mechanism. 12
Figure II.1: Illustration of general model illustration of the under-floor heating systems 16

List of tables

Table 1.1: Geometrical dimensions of the building components 23
Table 1.2: Thermo-Physique values of the building components 24
Table 2.1: Dimensions of the solar collector 25
Table 2.2:Operative thermo-physique parameters of the solar collector 25

List of Graphs

Graph 1: Outside ambient temperature…….....22
Graph 2: Solar radiation on a horizontal surface……23
Graph 3: Water temperature outlet of from copper collecteur…….....30
Graph 4: Water temperature outlet of from aliminum collecteur…….....30
Grape 5: Water temperature outlet of from copper collecteur…….....31
Graph 6: Water temperature outlet of from aluminm collecteur……31

Summary:

The present research study includes simple dynamic thermal energy model of a flat plate solar collector, connected to a radiant floor, in order to cover parametric studies about effective variables, contributed to performance increasing approach, for better heat supply of quality in residential building sector.

Key words:

Heat quality; Simple dynamic simulation; Flat solar collector; Radiant floor

Résumé :

Cette étude de recherche comprend un modèle dynamique simple d'énergie thermique d'un collecteur solaire à plaque plate, connecté à un sol radiant, afin de réaliser des études paramétriques sur les variables efficaces, contribuant à une approche d'augmentation des performances, pour un meilleur approvisionnement en chaleur de qualité dans le secteur du bâtiment résidentiel.

Mots clés :

Qualité de la chaleur ; Simulation dynamique simple ; Capteur solaire plat ; Plancher radiant

ملخص:

تتضمن الدراسة البحثية الحالية نموذجًا ديناميكيًا بسيطًا للطاقة الحرارية لجمع الطاقة الشمسية من الألواح المسطحة، المتصلة بأنظمة التدفئة الأرضية المشعة، بهدف إجراء دراسات برامترية حول المتغيرات الفعالة التي تسهم في زيادة الأداء، من أجل تحسين جودة إمدادات الحرارة في قطاع المباني السكنية.

الكلمات المفتاحية: جودة الحرارة؛ محاكاة ديناميكية بسيطة؛ جامع الطاقة الشمسية المسطح؛ بأنظمة التدفئة الأرضية المشعة.

Nomenclature :

A	Area (m²)
C	Specific heat capacity (J/kg·K)
D	Diameter (m)
G	Solar irradiance (W/m²)
K	Gain factor
Q	Energy consumption (MJ)
M	Mass (kg)
T	Temperature (°K or °C)
$\overline{T}$	Average temperature (°C)
T*	Predicted room air temperature (°K or °C)
U	Heat transfer coefficient (W/m²·K)
Db	Dead band temperature (°C)
dp	Distance between pipes (m)
hcomb	Combined heat transfer coefficient (W/m²·K)
hfc	Forced convection heat transfer
hr	Radiation heat transfer coefficient (W/m²·K)
hview	Heat transfer coefficient outside surface (W/m²·K)
k	Thermal conductivity (W/m·K)
ṁ	Fluid mass flow rate (kg/s)
tins	Insulation thickness (m)
tf	Floor thickness (m)
tgc	Glass cover thickness (m)
tgp	Air gap thickness (m)
tw	Wall thickness (m)
a	Percentage of solar irradiation (%)

Subscripts

abs	Absorber
amb	Ambient
btm	Bottom
buld	Building
cons	Consumption
des	Design
ec	Electrical equipment
exitf	Fluid exit
ext	External surfaces
fl	Floor
fld	Circulating fluid
fr	Inside floor surface to room
gc	Glass cover of the collector
gl	Window glass
gr	Ground
i	Node number
ifs	Inside floor surface
inf	Air infiltration
incol	Solar collector fluid inlet
inletf	Fluid inlet to the floor pipe
intub	Interior of the tube
inws	Inside mass wall surface
inw	Inside north wall surface
irf	Inside roof surface
iww	Inside west wall surface
j	Construction component
lat	Solar panel lateral side
oc	Occupants
ows	Outside wall surface
pl	Plate
pr	Plate to room
r	Room
ra	Room to outside air
rgl	Room to glazing
rmes	Measured room temperature
rmw	Room to mass wall
rnw	Room to north wall
rrf	Room to roof
rww	Room to west wall
set	Set point
si	Inside surface
so	Outside surface
sol	Solar irradiation

Greek Symbols

α	Diffusivity (m²/s)
Δt	Time step size (s)
ζ	Effectiveness
φ	Reflection coefficient
γ	Adaptive parameter
ϑ	Kinematic viscosity (m²/s)
ρ	Fluid density (kg/m³)
τ	Mass floor time constant (s)

General Introduction

General Introduction:

Among the most significant sources of renewable energy that have taken their place as promising alternatives to the traditional sources of energy is solar energy because it is free and permanently available not to mention that it is environmentally friendly. The past few decades have seen the world develop an increased interest in using technologies to tap into this energy and use it in a number of applications with the solar heating systems being the simplest and most common of all being the flat-plate solar collectors.

The objective of this thesis is to make a simplified dynamic simulation model of a flat plate solar collector attached to an underfloor heating system to investigate how physical and geometrical parameters influence the thermal performance of the system. Thanks to this simulation, it is possible to estimate the behavior of the system in real climatic conditions and under various operating conditions, which allows one to contribute to the efficiency of design and the choice of materials.

This work is rested on the comparative analysis of two solar collectors made of different absorber materials (copper and aluminum) and with different flow rates under semi-arid climate with the help of mathematical models according to the energy balance equations which are solved by the numerical method of finite difference.

Chapter I: Overview of Solar Thermal Systems

1. Introduction

1.1 Theoretical Bases:

The conversion of solar radiation into thermal, electrical, or chemical energy has become sustainable for energy systems. Solar energy is one of the major renewable energy sources alongside biomass, hydropower, and wind energy.

Thermal solar energy is the heat energy derived from solar radiation. It is captured to heat a fluid (liquid or gas). The energy received by the fluid can then be used directly (for domestic hot water, heating, etc.) through solar collectors of various designs.

Air flat-plate collectors transform the radiant energy from the sun into thermal energy extracted by the flowing air within the collector. This energy is utilized in various solar applications, such as drying grains or wood, heating industrial or residential spaces, and solar refrigeration, Joly 2018.

Several types of air collectors have been built and tested worldwide, with the main objective being to collect the maximum amount of solar energy at the lowest cost.

1.2 Flat-Plate Collectors:

These collectors have three main functions: to absorb solar radiation, to convert it into heat, and to transfer this heat to the heat transfer fluid. To maximize the absorption of solar radiation, a flat surface placed strategically is sufficient; this surface must have the highest possible absorption coefficient for the top layer.

1.2.1 Operating Principle of a Flat-Plate Solar Thermal Collector:

Solar water heating has received increased interest in recent years, primarily because it is a free energy source, and it is available, in principle, anywhere all over the world. The key element in a solar heating plant is the solar collector field, as it is at the collectors that the solar energy is captured and transferred to the circulating fluid. Currently, the collector type most widely used in such plants is the flat-plate solar collector, described by (Duffie and Beckman 2013).

The Figure 1a and 1b below represents a device that converts solar radiation into heat to transfer to a fluid. There are several types (unglazed collectors, glazed collectors, vacuum collectors), with the most common being the glazed flat-plate solar collector, which can achieve a heat transfer fluid outlet temperature of up to 100°C.

1.2.2 The principle of flat plate collector

A flat plate collector is a device acting as a heat exchanger. It converts solar power into thermal energy. It can gather solar energy and use it for heating systems, to heat water in the house for bathing, washing, etc. Also, it can be used to heat hot tubs and swimming pools.

Heating Solar collectors are usually described by stationary models that consider the collector to be in steady-state operation. Models have the advantage of being simpler and hence needing less computation time than dynamic models. However, this

simplification may be critical because solar collectors rarely reach a steady state during operation due to their large time constants and the variability of the driving forces. For several applications, e.g., the investigation of control strategies, it is desirable to take the collector dynamics into account (Guarracino, et al 2015).

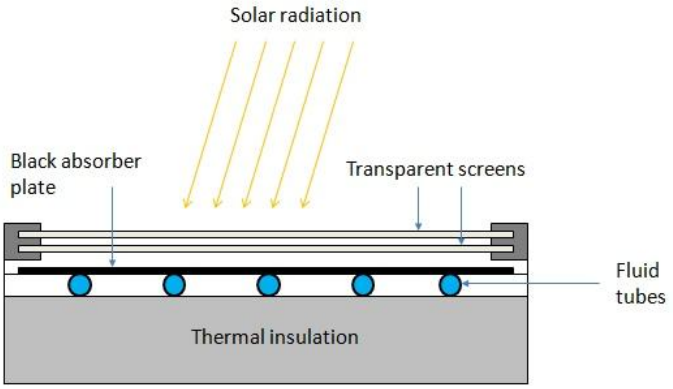

Figure I.1a: Schematic of a plate solar collector with transparent screens

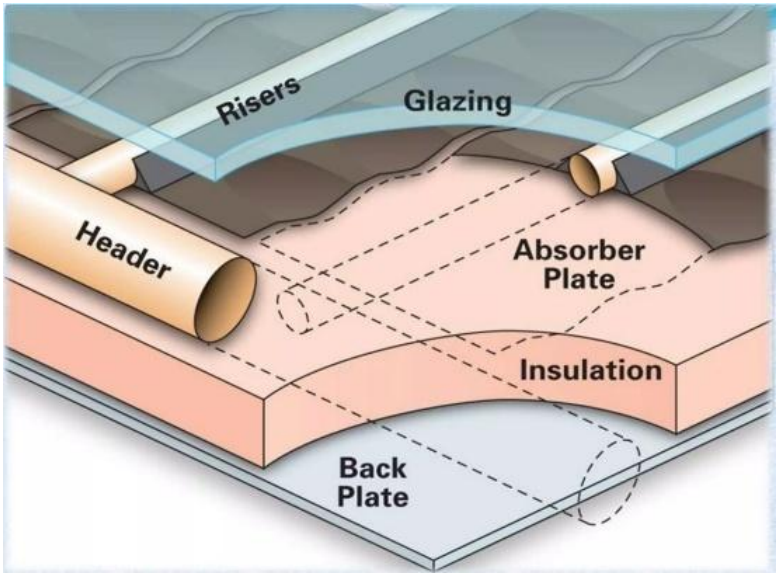

Figure I.1b: Components of solar flat plate collector

1.2.3 Glazed Flat Collector:

This is the most common model. It consists of an insulated casing covered by glazing. Inside is the absorber, a coil containing the fluid to be heated. To enhance heat absorption, the coil is surrounded by black fins, as the black color improves heat absorption.
In this type of model, the absorber is protected against thermal losses by an insulating material (usually rock wool). The glass is made of very strong tempered glass (resistant to weather and hail), highly transparent (low iron content), and specially designed to have a low reflection level to maximize heat capture (see Figure 1.a).

1.3 Different Components of the Solar Collector:

The flat solar collector essentially consists of the following elements:
An opaque plate that absorbs solar radiation and transmits it to the heat transfer fluid.
Thermal insulation at the back and sides.
A transparent cover usually made of single or double glass, which creates a greenhouse effect and prevents cooling of the absorber by protecting it from the wind.

1.3.1 The Absorber:

The absorber is a component of a thermal collector, such as a solar panel, that functions to absorb incident solar radiation and convert it into heat via a heat transfer fluid, aiming to achieve energy savings. The absorber is typically a black body that absorbs sunlight, mechanically connected or part of the same structure as a network that irrigates water. It can take the form of a metal plate, a glazed or unglazed coil, a vacuum tube, a plastic tarp, or a simple plastic/metal reservoir (Figure 2).

Two functions are assigned to the absorber:

- Absorb as much solar radiation as possible.
- Transfer the generated heat to the heat transfer fluid with minimal losses.

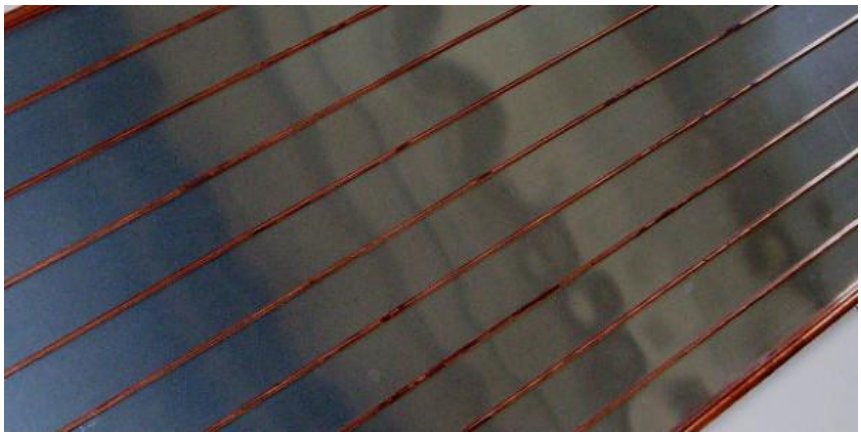

Figure I.2: Laser welding absorber.

1.3.2 The Transparent Cover:

The cover serves to protect the absorber, but it also plays an important role in the thermal balance by reducing heat losses. Typically, glass is used as a transparent cover.

1.3.3 The Thermal Insulator:

The thermal insulator limits heat loss, and its characteristic is the thermal conductivity coefficient; the lower it is, the better the insulator. The main materials used for thermal collectors are rock wool, glass wool, polyurethane foams, or melamine resin. More natural insulators are sometimes found.

In the case of glazed thermal collectors, it is also interesting to replace the insulation between the glass and the absorber with air. Indeed, air has a high insulating power and is thus used in double glazing. In pursuit of better performance, some manufacturers use other gases like argon or xenon, and when possible, even prefer a vacuum.

1.3.4 The Heat Transfer Fluid:

The heat transfer fluid is responsible for evacuating the heat stored by the absorber and transmitting it to where it needs to be consumed. A good heat transfer fluid must meet the following conditions:

- Be chemically stable at high temperatures, particularly during the stagnation of the collector.
- Have antifreeze properties correlated with local weather conditions.
- Have anticorrosive properties depending on the materials present in the collector circuit.
- Possess high specific heat and thermal conductivity to transport heat efficiently.
- Be non-toxic and have a low environmental impact.
- Have low viscosity to facilitate the circulation pump's task.
- Be easily available and inexpensive.

The best compromise regarding these criteria is a mixture of water and glycol (used in automobile cooling liquids), although it is not uncommon to find systems operating with pure water or simply air, depending on the application.
The fluid mass flow rate used for floor heating systems typically ranges from 0.5 to 1.5 liters per minute per square meter of heated surface area. This can vary based on system design, desired temperature, and specific heating requirements.
For precise calculations, factors such as is considered:

- Floor area: Total square meters to be heated
- Desired temperature rise: Difference between the supply and return fluid temperatures.
- Heat output requirements: Based on insulation and heat loss of the space

1.3.5 Tilt of a Solar Collector

The tilt of the collector should have an optimal angle based on the geographic coordinates of the location. The energy produced under real conditions will generally be significantly lower than that produced under standard conditions. It primarily depends on three factors:

- Daily Global Radiation: The amount of sunshine received.
- Ambient Temperature: The external temperature.
- Position of Solar Panels: Orientation and tilt.

A decrease in optimal tilt results in:

- A 10° deviation leads to about a 2% reduction in production.
- A 20° deviation results in a decrease of about 6%.
- A 30° deviation leads to a decrease of approximately 14%.

- A 40° deviation results in a nearly 25% decrease.

1.4 Types Solar Water Collector

There are two types of systems: low-pressure circulation systems and high-pressure circulation systems.

- Low-Pressure System: This system is used for heating pools, industrial water heating and domestic heating.
- High-Pressure System: In this system, the water circuit typically consists of copper tubes and a metal plate that increases the absorption surface. The fins are usually made of steel, aluminum, or copper, with thicknesses of about 0.25 mm for copper, 0.5 mm for aluminum, and 2 mm for steel, due to differences in thermal conductivity. The spacing between the tubes depends on the thickness of the fins.

1.4.1 Advantages and Disadvantages of Glazed Flat Collectors:

Advantages:

- **High Efficiency**: Glazed flat collectors have a good heat absorption capacity, making them efficient for heating applications.
- **Durability**: The use of tempered glass and robust materials ensures long-lasting performance.
- **Versatility**: Suitable for various applications, including residential and commercial heating systems.
- **Low Maintenance**: Generally, requires minimal maintenance over time.

Disadvantages:

- **Cost**: Initial installation costs can be relatively high compared to other collector types.
- **Thermal Losses**: Despite insulation, some heat loss can occur, especially during colder months.
- **Space Requirements**: Requires adequate space for installation, which might not be feasible in all locations.
- **Sensitivity to Weather**: Performance can be affected by extreme weather conditions, such as heavy snow or prolonged cloud cover.

1.4.2 Efficiency of a Solar Collector

The efficiency of a solar collector, designed to convert solar energy into thermal or photovoltaic energy, depends on its shape, the chosen technology, and how heat losses at its surface are minimized. There are two types of efficiency: optical efficiency and instantaneous efficiency.

The efficiency of a single-glazed flat plate solar collector can be calculated using the following formula:

$$\eta = \frac{Q_{useful}}{Q_{in}} \text{ x } 100$$

Where:

η = Efficiency of the solar collector (%)

Quseful = Useful heat output from the collector (W)

Qin = Incident solar radiation on the collector surface (W)

$$Q_{useful} = A.(I - L)$$

Where:

A = Area of the collector (m^2)

I = Incident solar radiation (W/m^2)

L = Heat losses from the collector (W/m^2)

Heat losses can be estimated using:

$$L = U.(T_{\text{collector}} - T_{\text{ambient}})$$

Where:

- U= Overall heat loss coefficient ($W/m^2 \cdot K$)
- Tcollector= Temperature of the collector (°C)
- TambientT = Ambient temperature (°C)

1.5 Bibliographic Studies

Modern solar energy techniques have led to the development of various solar water heating devices, which are being extensively researched for efficient residential energy use, (Schnieders, 1997) states that the flat-plate solar collector is the most commonly used in solar heating installations to meet the quantity and quality of thermal energy demand. When simulating these types of collectors using steady-state models, it can be crucial to note that solar collectors rarely reach a stable state during operation

due to their large time constants and the variability of driving forces. It is desirable for heating control strategies to take the dynamics of the collectors into account.

(Zima and Dziewa, 2011) proposed a one-dimensional mathematical model to simulate the transient processes occurring in liquid flat-plate solar collectors. The model was experimentally implemented and validated; the method takes into account the distributed parameters of the solar collector, particularly for: the glass cover, the air confined between the glazing and the absorber, the heating fluid used, and the insulation. The calculation results showed a satisfactory convergence of the measured and calculated fluid temperatures at the outlet of the collector. Other contributors, (Martinez. et al. 2005),((J. Cadafalch 2009) , Zhai. et al. 2009) have established their studies with the same methods of simplifications.

During the process of time, (A.M. Shariah et al. 1999) have examined the effect of thermal conductivity of the absorber plate in a thermosyphon and, find that Switching from steel to aluminum increases solar fraction by 4%–7% and characteristic factors by 12%–19%. Using copper instead of aluminum yields only a 1% increase in solar fraction and 3% in characteristic factors. Last decay, (R. Venkatesh and, W. Christraj, 2014) have investigated the thermal performance of multipurpose solar collectors, which enhance conventional solar water heaters by integrating riser tubes and headers. Experiments conducted on these systems, the results show that during summer performance, the multipurpose solar collector achieved a maximum daily average of 72.05% relative humidity, a mass flow rate of 0.0316 kg/sm², and wind speed of 0.873 m/s. During winter performance, The corresponding systems were significantly lower at 19.5% relative humidity, 0.0295 kg/sm² mass flow rate, and 0.722 m/s wind speed, with a minimum daily average of 11.23% relative humidity and 0.384 m/s wind speed. The results on solar water heater demonstrated higher heat removal (FR) and collector efficiency (Fo) factors compared to conventional systems in both seasons, particularly in summer. Also, the results indicate that the mass flow rate is influenced by solar radiation and relative humidity, showing that drier air leads to higher heat gain and water flow rates. (Mouna Hamed et al., 2014) presents a numerical investigation of flat plate solar collectors aimed at optimizing their performance and design for hot water supply. The system consists of three main components: a transparent cover, an absorber, and a transfer fluid. A transient simulation method was developed to analyze the dynamic behavior, establishing a model based on energy balance analysis. The model's equations were solved simultaneously to evaluate the impact of various parameters, including outlet water temperature and overall heat loss coefficient. More ever, a study was conducted by (G. A. Duvuna1 et al. 2019) to design a solar water heating system using MATLAB programming language. The study varied several design parameters to determine their effect on the system's solar fraction (f). The results showed that: Increasing the collector area and number of glazing increases the solar fraction (up to 97% with double glazing). Increasing the length of the collector tube increases the solar fraction. Decreasing the diameter of the tank increases the solar fraction (up to 75%). An air gap of 4.5-5 cm is suitable for optimal system performance. Decreasing the tube spacing increases the solar fraction. Increasing the plate thickness has a slight positive effect on the solar fraction (but is not cost-effective). The study provides insights into the effects of various design parameters on the performance of a solar water heating system.

1.6 Materials and Methods

Establishing a model from heat balance of single capacitance on each component of the solar panel, using improved and validated method of modelling by (Zima and Dziewa. 2011).

The model simulates a solar collector's transient process using constant physical properties, heat exchange surfaces, and geometrical dimensions. It considers four nodes representing single capacitance layers, including cover glass, air, absorber, and working fluid, Figure 2a and 2b.

The water solar panel model's differential equations are solved using the implicit finite-difference method, with time-dependent ambient conditions, solar radiation, and initial temperatures of 12°C.

The modeling implies a simplification of the real physical processes that occurs in the solar flate plate. These simplifications are made through the use of assumptions that allow the problem of heat transfer mechanisms to be solved more easily for example free convection heat exchange. Since the dynamic conditions of the model are being considered, the equations describing the heat transfer mechanism of the system are solved at every time step using the finite difference method. Their actions are simulated for a heating period of six months, under semi-arid weather conditions.

The parametric studies here in are atributed to heating homes by choosing single solar panel with differente absorber materials rnamely, alluminium and coper and with different water flow rate, to compare their thermal performances under winter arid climate .

The objective of the work aim to supply heat quality for different energy usage in residential building sector.

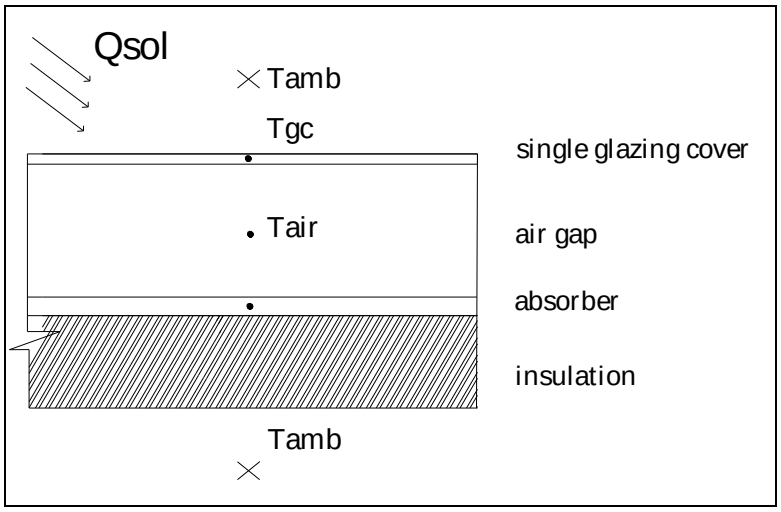

Figure I.2a: Single glazed flat plate solar panel temperature distribution.

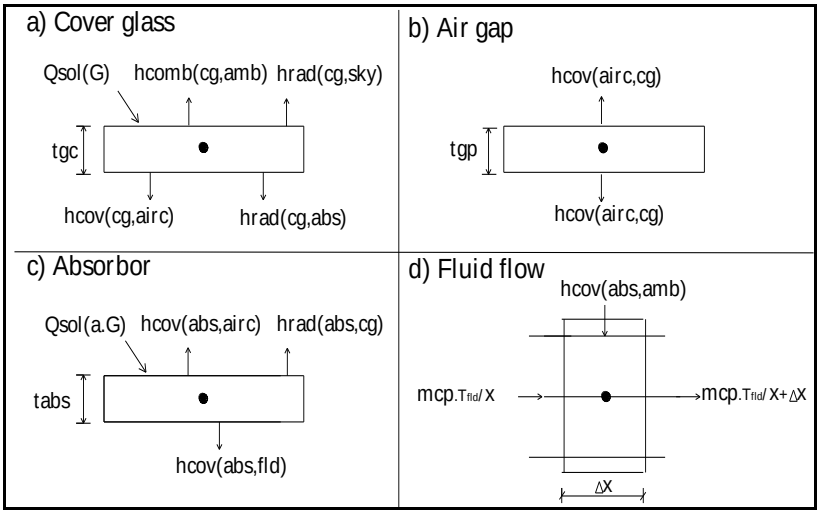

Figure I.2b: Single glazed flat plate solar panel heat mechanism.

Conclusion:

This chapter covers the theoretical principles related to flat plate solar collectors, in terms of their operating principle and basic components such as the absorber, glass cover, thermal insulation, and heat transfer fluid. It also discusses the types of collectors, their advantages and disadvantages, and the factors affecting their efficiency, particularly the angle of inclination and heat losses. In conclusion, the chapter presents a set of reference studies that addressed the modeling of the performance of these collectors using numerical methods, which form the scientific basis for building the model used in this study.

Chapter II: Simulation model of the solar flat plate

2. Numerical modeling of the active solar heting systems

2.1 The single glazing flat plate solar colector

2.1.1 Temperature calculations,

considering one node for each of the fore following components:

- ***Cover glass node*:**

$$\begin{pmatrix} Accumulted\ heat \\ in\ coverglass \end{pmatrix} = \begin{pmatrix} Heat\ loss \\ to\ the\ sky\ by\ \ radiation \end{pmatrix} +$$
$$+\begin{pmatrix} Heat\ loss \\ by\ convection\ to\ atmosphere \end{pmatrix}$$
$$+\begin{pmatrix} Heat\ transfer \\ from\ absorber\ plate\ by\ radiation \end{pmatrix}$$
$$+\begin{pmatrix} Heat\ transfer \\ from\ cover\ glass\ to\ air\ in\ the\ gab \end{pmatrix}$$
$$+\begin{pmatrix} Heat\ loss\ by\ lateral \\ faces\ of\ the\ cover\ glass \end{pmatrix}$$
$$+\begin{pmatrix} Incident\ solar \\ radiation \end{pmatrix}$$

Computed as:

$$M_{cg}cp_{gc}(dT_{cg}/dt) = A_{cg}[hr_{(cg,sky)}(T_{sky} - T_{cg}) + hc_{(cg,amb)}(T_{amb} - T_{cg})$$
$$+ hr_{(cg,abs)}(T_{abs} - T_{cg}) + hc_{(cg,air)}(T_{air} - T_{cg})$$
$$+U_{loss}.\nearrow^{0}.A_{(lat,cg)}(T_{amb} - T_{cg})$$
$$+A_{cg}(1 + \frac{\tau_{cg}(1-\alpha_{abs})}{1-\varphi_{cg}(1-\alpha_{abs})})\alpha_{gl}.G \qquad (1)$$

- **Air gap node between glass cover and absorber:**

$$\begin{pmatrix} Accumlted\ heat \\ in\ air\ gap \end{pmatrix} = \begin{pmatrix} Heat\ transfer\ by\ convection \\ from\ cover\ glass\ to\ air\ in\ the\ gab \end{pmatrix} +$$
$$+\begin{pmatrix} Heat\ transfer\ by\ convection \\ from\ absorber\ plate\ to\ air\ in\ the\ gab \end{pmatrix} + \begin{pmatrix} Heat\ loss\ by\ lateral \\ faces\ of\ the\ air\ gap \end{pmatrix}$$

Computed as:

$$M_{air}cp_{air}\left(\frac{dT_{air}}{dt}\right) = hc_{(cg,air)}A_{cg}\left(T_{cg} - T_{air}\right) + hc_{(abs,air)}A_{abs}(T_{abs} - T_{air}) + U_{loss}.\nearrow^{\mathbf{0}}.A_{(lat,amb)}(T_{amb} - T_{air}) \quad (2)$$

Absorber Node :

$$\begin{pmatrix} Accumlted\ heat \\ in\ absorber\ plate \end{pmatrix} = \begin{pmatrix} Heat\ loss \\ by\ \ radiation \end{pmatrix} + \begin{pmatrix} Heat\ loss \\ by\ convection \end{pmatrix} + \begin{pmatrix} Heat\ gain \\ by\ conduction \end{pmatrix} + \begin{pmatrix} Heat\ transfer \\ to\ working\ fluid \end{pmatrix} + \begin{pmatrix} Heat\ loss\ by\ lateral\ and \\ bootom\ sides\ of the\ collector \end{pmatrix} + \begin{pmatrix} Incident\ solar \\ radiation \end{pmatrix}$$

Computed as:

$$Mcp_{abs}(dT_{abs}/dt) = hr_{(cg,abs)}A_{cg}\left(T_{cg} - T_{abs}\right) + hc_{(abs,air)}A_{abs}(T_{air} - T_{abs}) + hc_{(abs,fld)}A_{(abs,fld}\left(T_{fld} - T_{abs}\right) + \left(U_{(loss,btm)} + U_{(loss,lat)}\right)\nearrow^{\mathbf{0}}.(T_{air} - T_{abs}) + A_{abs}\left(\frac{\tau_{cg}.\alpha_{abs}}{1-\varphi_{cg}(1-\alpha_{abs})}\right)G \quad (3)$$

- **Working fluid node:**

(Energy balance in a control volume of the working fluid) $=$
$\begin{pmatrix} Heat\ loss \\ by\ forced\ convection \end{pmatrix} + \begin{pmatrix} Heat\ transfer \\ to\ working\ fluid \end{pmatrix}$

Computed as:

$$(D_{in(tub)}/4)\rho_{fld}cp_{fld}\left(\left(\partial T_{fld}/dt\right) + \vartheta\partial T_{fld}/dx)\right) = hfc_{(abs,fld)}\left(T_{abs} - T_{fld}\right) + \dot{m}cp_{fld}(T_{fld} - T_{fld(floor\ inlet\ )}) \quad (4)$$

Heat loss through the pipe connection between the solar panel and the mass floor is considered negligible. Therefore, the fluid inlet temperature to the solar collector can be equated to the fluid exit temperature from the floor:

$$T_{fld(floor\ inlet)} = T_{fld(colector\ exit)}$$

The differential equations for the water solar panel model are solved using the implicit finite-difference method, accounting for time-dependent ambient conditions, solar radiation, and initial temperatures of 12 °C.

2.1.2 Model of the heated envelope

Building heating energy consumption is influenced by its envelope, heating plant efficiency, and control system quality, which connect the building to its heating system and inhabitants. The model in Figure 1 represents a single-zone building with solar under-floor heating systems. The building's west and north walls are mass less, while the east wall forms a mass wall. Hot water circulates through pipes in the mass floor, which is insulated on the bottom. Energy is transferred through air infiltration, solar gains, and heat losses. The model describes the long- and short-term dynamic characteristics of the system. Thermo-physical values of the building components are given by Karlekar and Desmond. The modelling approach involves creating a model for each system component based on its physical characteristics, calculating heat transfer using one-dimensional heat flow, and fitting parameter values for various configurations. The finite difference method is commonly used for simulating building models due to its flexibility and the availability of information.

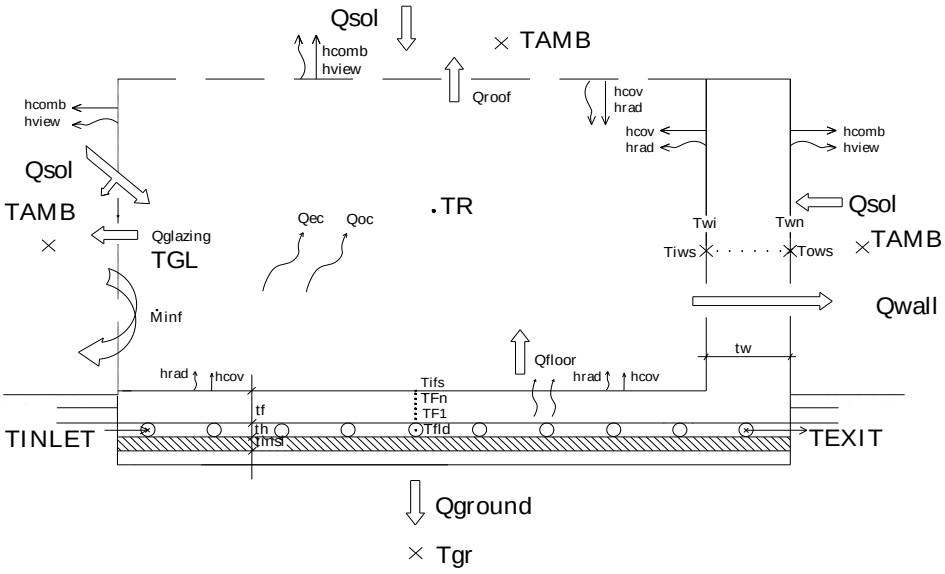

Figure II.1: Illustration of general model illustration of the under-floor heating systems (Typical of residence or office building)

2.1.3 Model development and Assumptions

The model is developed based on the following assumptions:

1. It considers long and short-wave radiation heat exchange.
2. It maintains thermal capacity for each air mass, floor, and wall.
3. It accounts for conduction through walls, floors, roofs, and glazing separately.
4. It accounts for air infiltration and ground heat losses.
5. The heat from inhabitants and electrical equipment has minimal impact on heat demand flexibility in small heating spaces and is neglected for the sake of simplicity.
6. It assumes negligible thermal resistances of surface pipes in the slab.
7. The effects of solar irradiation through the glazing are lumped onto the inside surfaces, including the air in the room, whereby each surface or air in the room is assumed to receive a fixed percentage of the solar gain.

2.1.3.1 Temperature calculations

- **Node Temperatures**

The fluid circulating through the embedded floor pipe is treated as a point source, represented by a single capacitive element with a temperature of T_{fld} ,the mass of the floor and the mass of the wall are divided into layers of thickness Δx_{fl} and Δy_w respectively. An energy balance for the time interval can be expressed as follows: the heat flux from all neighbouring nodes towards node i during Δt is equal to the increase in internal energy of the material associated with node i., i.e:

$$Mcp_i\left(\frac{T_i^{n+1}-T_i^n}{\Delta t}\right) = UA_{(i-1,i)}(T_{i-1}^n - T_i^n) + UA_{(i,i+1)}(T_{i+1}^n - T_i^n) \quad (5)$$

Rearranging the above equation to:

$$\left(\frac{T_i^{n+1}-T_i^n}{\Delta t}\right) = \frac{UA_{(i-1,i)}T_{i-1}^n + UA_{(i,i+1)}T_{i+1}^n}{Mcp_i} - \frac{(UA_{(i-1,i)}+UA_{(i,i+1)})T_i^n}{Mcp_i} \quad (6)$$

And letting: $\lambda_i = \left(UA_{(i-1,i)} + UA_{(i,i+1)}\right)T_i^n/Mcp_i$ (7)

$$\omega_i = T_i^{n+1}/\Delta t \quad (8)$$

$$S_i = \frac{UA_{(i-1,i)}T_{i-1}^n + UA_{(i,i+1)}T_{i+1}^n}{Mcp_i} \quad (9)$$

Equation (1) becomes: $(T_i^{n+1} - T_i^n/\Delta t) = \omega_i = S_i - \lambda_i T_i^n$ (10)

this equation can be written as: $T_i^{n+1} = (1 - \lambda_i \Delta t)T_i^n + S_i \Delta t$ (11)

In the case of the simulation model, the maximum permissible time step size is found to be equal 2.5 seconds, which is, too time consuming for a long-term simulation. However, an increase in permissible time step size can be achieved without loss of accuracy, by introducing a weighting factorσ_i , i.e choosing an implicit solution.

Equation (1) becomes: $T_i^{n+1} = T_i^n + \sigma_i \omega_i \Delta t$ (12)

Solving forω_i, we get $\omega_i = \frac{S_i - \lambda_i T_i^n}{1 + \lambda_i \sigma_i \Delta t}$ (13)

the weighting factor σ_i is found from matching the analytical and the implicit numerical equations

of ω_i, namely: $\frac{(1 - e^{-\lambda_i \Delta t}) S_i - \lambda_i T^n}{\lambda_i T^n} = \frac{S_i - \lambda_i T_i^n}{1 + \lambda_i \sigma_i \Delta t}$ (14)

Solving for σ_i we get: $\sigma_i = \frac{1}{(1 - e^{-\lambda_i \Delta t})} - \frac{1}{\lambda_i \Delta t}$ (15)

From this equation, σ_i always takes values in the range **[0,1]** whatever the value of the product $(\lambda_i \Delta t)$. Once ω_i is computed, the predicted temperature of nod i for a time step size Δt is given

as: $T_i^{n+1} = T_i^n + \omega_i \Delta t$ (16)

The same procedure outlined above is used to calculate each nodal temperature for the working fluid, mass floor, mass wall, and air in the room. The model simulation of the system is implemented in computer code using a modular programming approach. The initial value for each temperature is 12 °C, which is an estimated mean average temperature for the starting day of the simulation.

- **Surface temperatures**

A steady-state energy balance on each of the inside and outside of the building is used to calculate their temperatures. The surface temperature equation can be expressed in terms of conductive, convective, and radiation heat exchange, including the solar heat gains on the outside surfaces of the heated envelope. The inside surfaces or the room air are assumed to receive a fixed percentage of the gain. The glazing is assumed to have only one surface temperature since its thickness is chosen to be small.

A steady state energy balance on each of the inside and the outside building is used to calcuate their temperatures. The surface temperature equation can be expressed in terms of conductive, convective and radiative heat exchange, including the solar heat gain on outside envelope surfaces. The inside surfaces or the room air are assumed to receive a fixed percentage of the gain. The glazing is assumed to have only one surface temperature since its thickness is chosen small (5 mm).

$T_{si} = \frac{\sum (UA_j . T_j) + a_{sol} . G}{\sum UA_j}$ (17)

$T_{so} = \frac{\sum (UA_j . T_j) + G}{\sum UA_j}$ (18)

- **Room air temperature**

The room air temperature is defined as the process output that must be controlled. This temperature results from the heat input through the floor, solar irradiation, and heat losses through the mass wall, glazing, roof, remaining walls, and air infiltration. Therefore, the variation of room air temperature can be seen as dependent on the following physical quantities, defined as process inputs: the inlet fluid temperature, the fluid mass rate entering the heating element, outside air temperature, solar irradiation, and wind velocity. The existence of non-measurable disturbances is not taken into account.

$$S_r = (UA_{(fl,r)}T_{ifs} + UA_{(r,mw)}T_{imws} + UA_{(r,rf)}T_{irf} + UA_{(r,gl)}T_{gl} + UA_{(r,nw)}T_{irnw} + UA_{(r,ww)}T_{iww} + \dot{m}_{inf}cp_{air}T_{amb} + a_{sol}G + Q_{oc}\nearrow^{\mathbf{0}} + Q_{ec}\nearrow^{\mathbf{0}})/Mcp_{air}$$

$$\lambda_r = (UA_{(fl,r)} + UA_{(r,w)} + UA_{(r,rf)} + UA_{(r,gl)} + UA_{(r,nw)} + UA_{(r,ww)} + \dot{m}_{inf}cp_{air}) \quad (19)$$

$$\sigma_r = \frac{1}{(1-e^{-\lambda_r.\Delta t})} - \frac{1}{\lambda_r \Delta t} \quad (20)$$

$$\omega_r = \frac{S_r - \lambda_r T_r^n}{1+\lambda_r \sigma_r \Delta t} \quad (21)$$

$$T_r^{n+1} = T_r^n + \sigma_r \omega_r . \Delta t \quad (22)$$

- **Temperature output of fluid from embedded pipes:**

The heat input to the floor from the solar plate can be expressed as:

$$Q_{cons} = \zeta \dot{m} cp_{fld}\left(T_{fld(inlet)} - T_{fld(outlet)}\right) \quad (23)$$

Where ζ is the effectiveness of heat element given by $\zeta = 1 - e^{-NTU}$ (24)

$$NTU = \frac{UA_{(fld,fl)}}{\dot{m}cp_{fld}} \quad (25)$$

Q_{cons} can also be expressed as: $Q_{cons} = \dot{m}cp_{fld}\left(T_{fld(inlet)} - T_{fld(outlet)}\right)$ (26)

By matching the two expressions of Q_{cons}, we get the temperature of the fluid as a function of the inlet temperature and the temperature of the first-floor node:

$$T_{out(fld)} = \zeta T_{fl(1)} + (1-\zeta)T_{fld(inlet)} \quad (27)$$

2.1.3.2 Heat transfer coefficient calculations

The linearization assumption is used for long-wave radiation heat transfer between internal surfaces and surrounding surfaces. Correlations for free convection heat transfer in real-sized three-dimensional enclosures are provided by (Khalifa and Marshall 1990). Ground heat losses are calculated using a commonly employed method, (Boileau and Latta 1968).

- **Free convection exchange between the glass and the outside environment:**

$$h_{comb(gl,ext)} = 3.8v_{vind} + 5.62 \quad \text{(Green 1984)} \tag{28}$$

- **Free convection exchange between the glass and the confined air:**

$$h_{c(gl,airgap)} = Nu.2.\lambda_{airc}/b$$

- **Free convection exchange between the confined air and the absorber:**

$$h_{c(,airgap,absor)} = Nu.2.\lambda_{airgap}/b$$

$h_{c(gl,airc)}$ et $h_{c(,airgqp,absor)}$ are calculated using the same values of Nu and Gr.

Following correlation proposed for the calculation of the Nusselt number, (Duffie and Backman 1981).

$$Nu = \left[0.006 - 0.017\left(\frac{\beta}{90}\right)\right].Gr^{1/3}. \tag{29}$$

$$Gr = \frac{g.(T_{absr}-T_{gl})}{\vartheta^2 T_{ext}} b^2 \tag{30}$$

where:

β: angle of inclination of the sensor relative to the horizontal.

λair: thermal conductivity of air.

ϑ: kinematic viscosity.

b: distance between the glass and the absorber.

g: gravitational acceleration.

❖ **Convection exchange between the tube (or the insulation) and the heat transfer fluid:**

The applied correlations are:

- Laminar flow: $(\mathrm{Re} < 2100)$

$\mathrm{Gz} < 100$:

$$\mathrm{Nu} = 3.66 + \frac{0.085.\mathrm{Gz}}{1+0.047\mathrm{Gz}^{2/3}}\left[\frac{\mu_f}{\mu_p}\right]^{0.14} \quad (31)$$

Pour $\mathrm{Gz} > 100$:

$$\mathrm{Nu} = 1.86.\,\mathrm{Gz}^{1.3}\left[\frac{\mu_f}{\mu_p}\right]^{0.14} + 0.87(1 + 0.015\mathrm{Gz}^{1/3} \quad (32)$$

- transient flow. Ou: $(2100 < \mathrm{Re} < 10000)$

$$\mathrm{Nu} = 0.116(\mathrm{Re}^{2:3} - 125)\mathrm{Pr}^{\frac{1}{3}}\left(1 + \left(\frac{\mathrm{D}}{\mathrm{L}}\right)^{\frac{2}{3}}\right).\left[\frac{\mu_f}{\mu_p}\right]^{0.14} \quad (33)$$

- turbulent flow: $\mathrm{Re} > 10000$

$$\mathrm{Nu} = 0.023.\,\mathrm{Re}^{0.8}\,\mathrm{Pr}^{1.3}\left[\frac{\mu_f}{\mu_p}\right]^{0.14} \quad (34)$$

with:

$\mathrm{Re} = \mathrm{v}\,.\,\mathrm{D}/\nu$ (dimensionless Reynolds number) (35)

$\mathrm{Gz} = \mathrm{Re}.\,\mathrm{Pr}.\,\mathrm{D}/\mathrm{L}$ (dimensionless Grashof number) (36)

where:

ρ: Density.

$\overline{v}_{fld}$: Average fluid velocity.

D: Tube diameter.

μ: Dynamic viscosity.

ν: Kinematic viscosity.

L: Tube length.

μ_f : Dynamic viscosity of water at the considered temperature.

μ_p: Dynamic viscosity of water at the wall at the considered temperature.

so:

$$h_{cov(absr,fld)} = Nu.\lambda_{copper}/e_{tub} \quad (37)$$

$$h_{cov(absr,iso)} = Nu.\lambda_{iso}/e_{iso} \quad (38)$$

e_{tub} et e_{iso} being respectively the thicknesses of the tube and the lower insulation of the collector.

- **Radiative exchange between the glass and the sky:**

$$h_{rad(gl,ciel)} = \varepsilon_{ver}\sigma\left(T_{gl}^{\ 2} + T_{sky}^{\ 2}\right)\left(T_{ver} + T_{sky}\right) \quad (39)$$

where: σ Stefan-Boltzman constant = 5.678 x 10^{-8}W. m^{-2}. K^{-4}

ε_{gl} is the emissivity of the ordinary glass cover

The heat transfer coefficient through the exterior surfaces viewed by the sky: Or the temperature of the sky is expressed by a simple relationship that links the temperature of the sky to the local outdoor air temperature given by (Swinbank.1963)

$$T_{sky} = 0.0552.T_{ext}^{\ 3/2} \qquad (T_{sky} \text{et } T_{ext}) \text{ en (°K)} \quad (40)$$

- **Radiative exchange between the glass and the absorber:**

$$h_{rad(gl,absr)} = \frac{\sigma\left(T_{gl}^{\ 2}+T_{absr}^{\ 2}\right)\left(T_{sky}+T_{absr}\right)}{\frac{1}{\varepsilon_{gl}}+\frac{1}{\varepsilon_{absr}}-1} \quad (41)$$

ε_{absr} is the emissivity of the absorber.

2.2 Numerical application:

Wheater data is given in Graph 1 and 2 for semi arid weather condition of seven continuos cold day stating from the January the 1st . this type of climate is carateriased by high temperature flectuations.

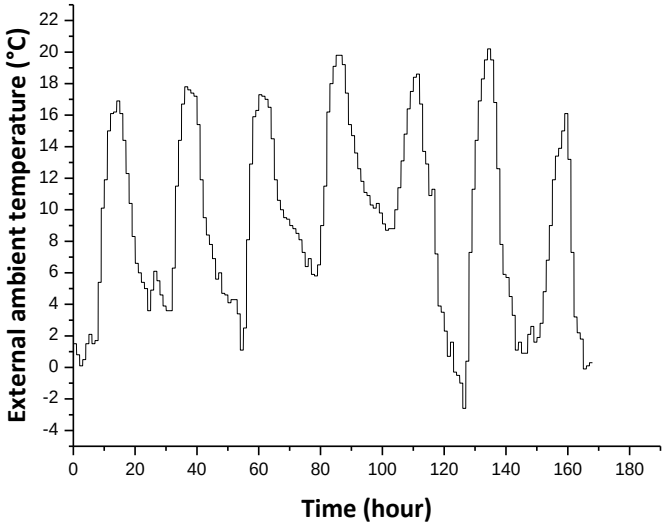

Graph 1: Outside ambient temperature

(7 consecutive cold days)

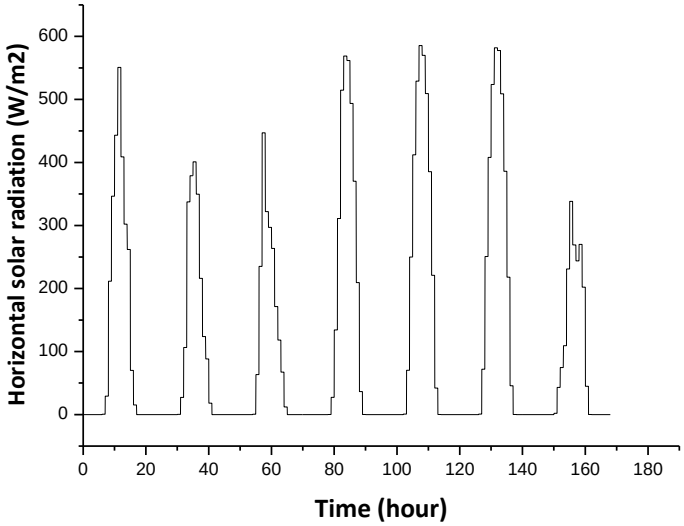

Graph 2: Solar radiation on a horizontal surface

(7 consecutive cold days)

Table 1.1: Geometrical dimensions of the building components

Elements		Dimensions	Units
Enveloppe volume (X * Y * Z)	V	6 * 4 * 3,5	m^3
Floor mass surface	A_{fl}	0.24	m^2
Floor mass thickness	t_{fl}	0.30	m
Pipe diameter	d_{cd}	0.022	m
Pipe thickness	t_{cd}	0.002	m
Distance between pipes	lc	0.02	m
Floor insulation thickness	t_{iso}	0.05	m
East wall (Y * Z) (mass wall)	A_{Ew}	4 *3.5	m^2
East wall thickness	t_{msw}	0.20	m
Nord wall (X * Z)	A_{Nw}	6*3.5	m^2
West wall (Y * Z)	A_{Ww}	4 *3.5	m^2
North and West walls thickness	t_w	0.10	m
South oriented glazing (X * Z)	A_{gl}	3 * 2,5	m^2
Glass thickness	t_{gl}	0.005	m
Roof (X * Y)	A_{rf}	6 *4	m^2
Roof thickness	t_{rf}	0.15	m

Table 1.2: Thermo-Physique values of the building components

Elements	Thermo-Physique values		
Room air	λ_{air}	0,0251	W/m °K
	ρ_{air}	1,164	kg/m^3
	cp_{air}	1012,18	J/kg °K
	ϑ_{air}	18,24E-6	m^2/s
Floor slab (heavy concrete)	λ_{fl}	1.4	W/m °K
	ρ_{fl}	2000	kg/m^3
	cp_{fl}	880	J/kg °K
	ε_{fl}	0.95	/
Heating fluid (water glycol at 20 °C)	λ_{fld}	0,624	W/m °K
	ρ_{fld}	995.33	kg/m^3
	cp_{fd}	4178.8	J/kg °K
	ν_{fd}	0.7 E-6	m^2/s
	Pr	4.68	/
Insulation (Board fiber)	cp_{ins}	237.1	J/kg °K
	ρ_{ins}	20	kg/m^3
	λ_{ins}	0,04	W/m °K

Wall (Brick dry)	λ_w ρ_w cp_w $\varepsilon_{w(int)}$ $\varepsilon_{w(ext)}$	0.52 1810 840.0 0.2 0.01	W/m °K kg/m³ J/kg °K / /
Roof (Roofing brick)	λ_{rf} ρ_{rf} cp_{rf} $\varepsilon_{rf(int)}$ $\varepsilon_{rf(ext)}$	0,8 1810.0 840.0 0.2 0.01	W/m °K kg/m³ J/kg °K / /
Pipe (PER)	λ_{cd}	0,35	W/m °K
Glazing (Ordinary glass)	λ_{gl} ε_{gl} α_{gl}	0,76 0.9 0.05	W/m °K / /

Table 2.1: Dimensions of the solar collector

Element	**Dimensions**		
Simple cover glass	A_{cg} nb_{cg} e_{cg}	1.60 1 0.005	m^2 / m
Glass-Absorber distance	$dis_{(cg,absr)}$	0.02	m
Absorber - Tubes - Welding	A_{abs} $d_{int(abs)}$ $d_{ext(abs)}$ nb_{tub} dis_{tub} e_{wld} l_{wld}	1.60 0.018 0.02 10 0.018 0.005 0.02	m^2 m m / m m m
Insulation	A_{lat} A_{btm} A_{bac}	0.60 0.60 1.60	m^2 m^2 m^2

Table 2.2: Operative thermo-physique parameters of the solar collector

Element	**Thermo-Physique values**		
Ordinary glass	cp_{gc}	840	J/kg °K
	ρ_{gc}	2700	kg/m^3
	λ_{gc}	0.93	W/m °K
	τ_{gc}	0.92	/
	α_{gc}	081	/
	ε_{gc}	0.94	/
	K_{gc}	0.28	/
Confined air	cp_{air}	1300	J/Kg °K
	ρ_{air}	1.2	Kg/m^3
	λ_{air}	0.025	W /m °K
Absorber with - Black selective layer - Cooper tube - Weld	cp_{cu}	398.0	J/Kg °K
	ρ_{cu}	8900	Kg/m^3
	λ_{cu}	386.0	W /m °K
	α_{cu}	0.88	/
	ε_{abs}	0.15	/
	λ_{wld}	5.0	W /m °K
Absorber with - Black selective layer - Alimunium tube - Weld	cp_{al}	230.0	J/Kg °K
	ρ_{al}	2700	Kg/m^3
	λ_{al}	230.0	W /m °K
	α_{al}	0.07	/
	ε_{abs}	0.15	/
	λ_{wld}	5.0	W /m °K
Fluid (Water glycol)	cp_{fld}	4178.8	J/Kg °K
	ρ_{fld}	1.0	Kg/m^3
	λ_{fld}	1.00,624	W /m °k m^2
	ϑ_{fld}	$0.7\ E-6$	m^2/s
	Pr	4.68	/
Insulation (Expanded Polystyrene)	cp_{ins}	1500	J/Kg °K
	ρ_{ins}	20.0	Kg/m^3
	λ_{ins}	0.04	W /m. °K

Conclusion:

This chapter presents the numerical model used to simulate the dynamic performance of a flat plate solar collector connected to an underfloor heating system. The model was built based on the energy balance equations for the system components (glass, air, absorber, and fluid), using the finite difference method to solve the differential equations. The modeling also included the effect of the building envelope and heat losses through walls and roofs, in addition to studying the effect of fluid properties and flow rate. This numerical representation allows for the evaluation of the thermal performance of the system under real climatic conditions and the analysis of influencing variables before moving on to the applied study in the next chapter.

Chapter III: Results and Discussions

3. Results and Discussions:

Focusing on the performance of solar panels under specific climatic conditions, particularly on two different absorber materials (copper and aluminum) and their thermal efficiency in heating water, with two different amount of the fluid mass rate, 0.36 kg/s 0.72 kg/s. for 7 consecutive cold days

First setup (0.36 kg/s fluid mass rate):

Under semi-arid climatic conditions for the coldest consecutive 7 days in January, the flat solar panel with ordinary single glazing, featuring a copper absorber with a selective coating of 200 μm, and fluid mass rate of 0.36 kg/s, has a significant influence on the exposure of the temperature regulation element by increasing the efficiency of the collector by 0.93. This setup produces quality hot water without causing overheating, with a maximum average temperature reaching 70°C. Consequently, the result is appropriate adaptation for the thermal regulation of the system, with a solar panel area of 1.60 m² and a 6% capture ratio

The selection with an aluminum absorber with a selective coating of 200 μm, with the same fluid mass rate, reaches maximum average temperatures of 50°C and 40°C, respectively, leading to more significant temperature drops to an average of 21°C, compared to the first combination, giving efficient of 84, as shown in

Graph 3 and 4.

Emphasised result:

With Copper Absorber:

Fluid mass rate of 0.36 kg/s

- Significant influence on temperature regulation.
- Increases collector efficiency by 0.93.
- Produces quality hot water without overheating.
- Maximum average temperature: 70°C.
- Appropriate adaptation for thermal regulation.
- Panel area: 1.60 m².
- Capture ratio: 6%.

Aluminum Absorber:

- Maximum average temperatures: 50°C and 40°C.
- More significant temperature drops (average of 21°C) compared to copper.

Efficiency of 84.

Fluid mass rate of 0.72 kg/s fluid mass rate

- (Higher fluid mass rate results in efficiency reduction: 0.90 for copper and 0.80 for aluminum.

Second setup:

Simulating the heat exchange for same precedent combination with a double fluid mass rate of 0.72 kg/s, the results are shown in Graph 5 and 6 , indicates that delivering heat with higher fluid mass rate result in efficiency reduction of 0.90 and 0.80 for both copper or aluminum absorbers respectively.

Concluding that: The copper-based system achieves a maximum average temperature of 70°C, indicating high efficiency in converting solar energy to heat.

In contrast, the aluminum absorber configuration achieves lower maximum average temperatures (50°C and 40°C), suggesting reduced efficiency.

The copper system is noted for its ability to produce quality hot water without overheating, which is crucial for practical applications.

The mention of significant temperature drops in the aluminum system (to an average of 21°C) highlights its inferior performance compared to the copper system.

Evaluation of the result:

With Copper Absorber:

Fluid mass rate of 0.36 kg/s

- Significant influence on temperature regulation.
- Increases collector efficiency by 0.93.
- Produces quality hot water without overheating.
- Maximum average temperature: 70°C.
- Appropriate adaptation for thermal regulation.
- Panel area: 1.60 m².
- Capture ratio: 6%.

Aluminum Absorber:

- Maximum average temperatures: 50°C and 40°C.
- More significant temperature drops (average of 21°C) compared to copper.
- Efficiency of 84.

Fluid mass rate of 0.72 kg/s fluid mass rate

- (Higher fluid mass rate results in efficiency reduction: 0.90 for copper and 0.80 for aluminum.

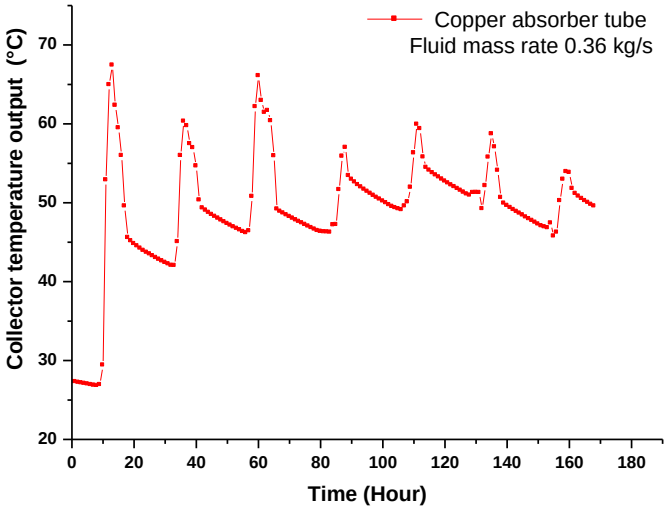

Graph 3: Water temperature outlet of from copper collecteur

(Short term simulation of cold continious 7 days)

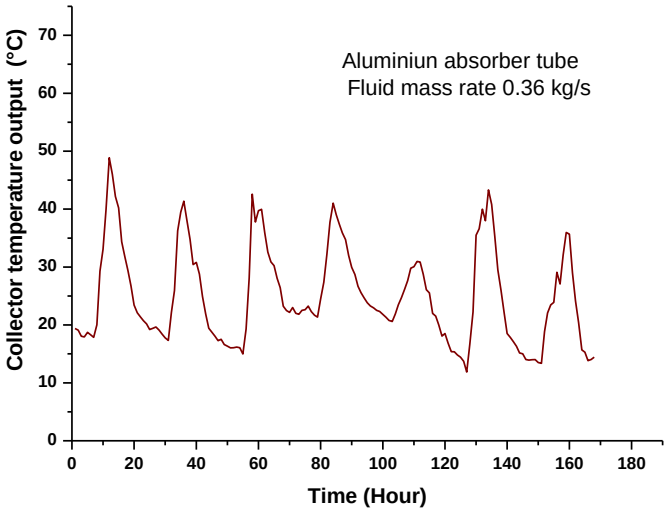

Graph 4: Water temperature outlet of from aliminum collecteur

(Short term simulation of cold continious 7 days)

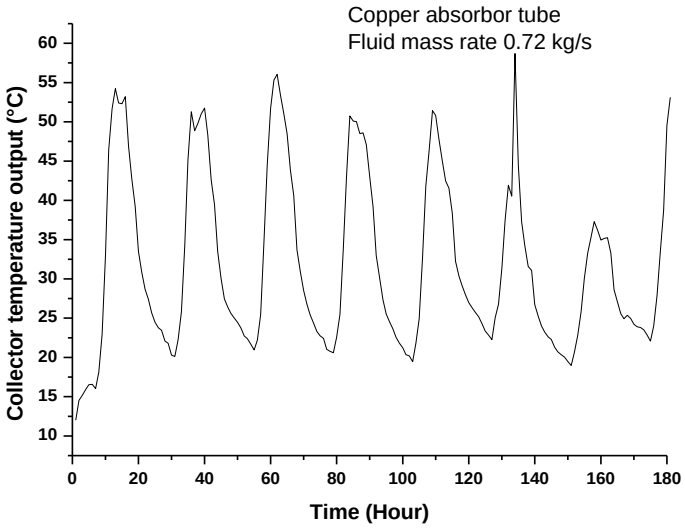

Graph 5: Water temperature outlet of from copper collecteur

(Short term simulation of cold continious 7 days)

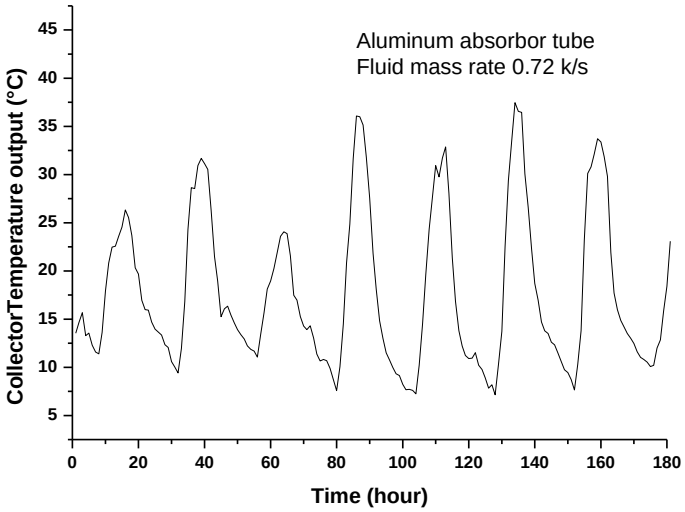

Graph 6: Water temperature outlet of from aluminm collecteur

(Short term simulation of cold continious 7 days)

GENERAL CONCLUSION

GENERAL CONCLUSION

General conclusion:

- The model developed in this thermo-mechanical parametric study describes the short- and long-term dynamic characteristics of a flat solar collector. The approach used for modeling involves establishing a model for each component of the collector based on its physical characteristics. Heat transfer through the system is calculated assuming one-dimensional heat flow. The values of the parameters are determined to match the model for a variety of different configurations.

  The finite difference method is applied in the simulation to evaluate the temperature distribution at each time interval. The simulation model is implemented in a computer code, and test steps are performed to identify the thermodynamic behavior of the simulated collector.
- **Copper-based system:** Achieves a maximum average temperature of 70°C, indicating high efficiency in converting solar energy to heat.
- **Aluminum absorber:** Achieves lower maximum average temperatures (50°C and 40°C), suggesting reduced efficiency.
- **Copper system:** Produces quality hot water without overheating, which is crucial for practical applications.
- **Aluminum system:** Significant temperature drops (to an average of 21°C) highlight its inferior performance compared to the copper system.

Consequently, the parametric study concluded that the flat solar collector with single glazing and a copper absorber selection ensures good thermal adaptation, and provides a higher yield compared to other types of combinations, suggesting practical implications for design choices.

Reference

Boileau GG, Latta JK. Simplified method based on heat transfer paths to ground, *ASHRAE* 1968. Google Scholar

Cadafalch, J**,** A detailed numerical model for flat-plate solar thermal devices, Solar Energy 2009,V83, 12, , Pages 2157-2164
doi.org/10.1016/j.solener.2009.08.013

Duffie, J.A , Beckman, W.A, Solar Engineering of Thermal Processes, John Wiley & Sons 2013 Book

Duvuna1, G. A., Tashiwa, Y. I., Zhigilla, Y. I., Parametric study of an active solar flat-plate collector water heater, Nigerian Journal of Technology (NIJOTECH) 2019, V 38(4), 876 – 883
https://dx.doi.org/10.4314/njt.v38i4.9

Green, A.A., The influence of operating conditions on the thermal performance of non-concentrating, solar collectors. Phd, Thesis, University College Cardiff, UK 1984.

Guarracino,I., Freeman, J., Markides, CN., Dynamic Testing and Modeling of Solar Collectors Conference: 14th UK Heat Transfer Conference 2015

Hamed, M , Fellah, A , Ben Brahim, A , Parametric sensitivity studies on the performance of a flat plate solar collector in transient behavior, Energy Conversion and Management 2014 78:938-947
https://doi.org/10.1016/j.enconman.2013.09.044

Joly, J.P, Energie solaire, les bases théoriques pour la comprendre Encyclopédie de l'Energie 2018
https://www.encyclopedie-energie.org/rubriques_articles/bases-theoriques/

Marti´nez , PJ., Vela´zquez, A., Viedma, A., Performance analysis of a solar Energy-driven-heating-system, Energy and Buildings 2005,37(10) 1028-1034.
doi.org/10.1016/j.enbuild.2004.12.008

Shariah, A.M., Rousan, A., Rousan Kh.K., Ahmad, A.A., Effect of thermal conductivity of absorber plate on the performance of a solar water heater Applied Thermal Engineering 1999**,** 19(7), 733-741
https://doi.org/10.1016/S1359-4311(98)00086-6

Swinbank, W.C., (1963) Long-Wave Radiation from Clear Skies, the Royal Meteorological Society, 89, 339-348. 1963

Venkatesh, R., Christraj, W., Performance Analysis of Solar Water Heater in Multipurpose Solar Heating System
Applied Mechanics and Materials 2014, (V592-594), 1706-1713.
https://doi.org/10.4028/www.scientific.net/AMM.592-594.1706

Zhai, X.Q., Yang, J.R., Wang, R.Z., Design and performance of the solar-powered floor heating system in a green building, Renewable Energy 2009,34 1700-1708.
doi.org/10.1016/j.renene.2008.11.027

Zima, W., Dziewa, P.,Modelling of liquid flat-plate solar collector operation in transient states, Proc. of the Institution of Mechanical Engineering Part A: Journal of Power and Energy 2011, 225 (1) 53-62.
doi.org/10.1177/09576509JPE1044